JOURNAL OF MATERIALS SCIENCE 22 (1987) 170–176

Particle distribution control in cast aluminium alloy–mica composites

DEO NATH
Department of Metallurgical Engineering, Institute of Technology, Banaras Hindu University, Varanasi 221 005, India

RAJIV ASTHANA, P. K. ROHATGI
Regional Research Laboratory, Hoshangabad Road, Habibganj Naka, Bhopal, India

A suspension of mica particles (40 μm diameter and 3.7 μ thick) obtained in a mechanically stirred Al–4 wt% Cu–1.5 wt% Mg melt was poured and solidified in a variety of moulds under different heat flow configurations. The resulting cast structure showed a non-uniform distribution of dispersed mica particles with mica-depleted and segregated zones due to their flotation before and during solidification. The experimentally observed profiles of mica-free regions deviate significantly from those computed on the basis of Stokes's law and freezing-time computations. In relatively thick castings, segregation of mica could be minimized by using low pouring temperatures and/or side as well as bottom chilling. It was found, however, that thin castings (12.5 mm) could easily be produced with a homogeneous distribution of mica particles.

1. Introduction

Mica particles dispersed in metallic matrices [1–7] result in particulate composites suitable for anti-friction applications. The conventional method of making these composites is the relatively costly powder metallurgy technique, which can produce smaller parts of relatively simple shapes. The casting technique of making particulate composites is much cheaper than powder metallurgy, and can produce larger parts of even complicated shapes. The process involves obtaining a suspension of particles in liquid alloy, followed by pouring and solidifying it in suitable moulds. The cast composites obtained by this process generally show segregation of particles in the region which is last to solidify due to the movement of particles during solidification. Such segregation has been found by the authors to be useful for certain applications [8]. The segregation may result from several factors including flotation of lighter particles, fluid convection due to the momentum of pouring and thermal gradients, flocculation of particles, and their rejection by the moving solid–liquid interface. This paper demonstrates the relative significance of some of these factors in determining the particle distribution and explains why simple flotation laws cannot by themselves account for the observed discrepancy between theory and experiment. Finally, it also demonstrates how a uniform distribution of mica particles in cast composites can be obtained by suitably controlling the solidification parameters (pouring temperature, thickness of casting and use of chills etc.).

2. Experimental procedure

About 2 to 3 kg batches of Al–4 wt% Cu alloy were melted in a super-salamander clay–graphite crucible (Khandelwal Crucibles and Mineral Industries, Rajamundry, India) in an oil-fired furnace. The crucible was kept in an electrical resistance holding furnace and the melt was degassed by bubbling nitrogen into it. About 1.5 to 2.0 wt% mica powder and magnesium pieces were added simultaneously into a vortex created by mechanically stirring the melt at 1000 r.p.m. Stirring was continued for about half a minute after the powder addition was over and the melt was then degassed by bubbling nitrogen at a slower rate. The degassing was accompanied by stirring at 500 r.p.m. for about 1 min after which it was stopped, the stirrer taken out of the melt and the crucible removed from the furnace. The melt was hand-stirred with a graphite rod before being poured into various moulds; the pouring temperature was 700° C in most cases. A detailed description of the process is given elsewhere [9].

The different kinds of mould used in the present study were as follows:

1. Moulds used to study the flotation and segregation of mica particles:

(i) Cast iron moulds with 50 and 65 mm internal diameter, 20 mm wall thickness and 200 mm height.

(ii) Sand moulds with cooling arrangement as shown in Figs 1a and b. The mould shown in Fig. 1a had a water-cooled copper chill at the bottom and was poured from the top, whereas the mould shown in Fig. 1b was bottom-poured and had a heavy copper chill at the top. This mould had a pouring cup, the upper level of which was 80 mm above the top of the mould cavity.

(iii) A steel mould with 80 mm internal diameter, water-cooled from the sides as shown in Fig. 2a.

(iv) A cast iron rotating mould mounted on the

0022–2461/87 $03.00 + .12

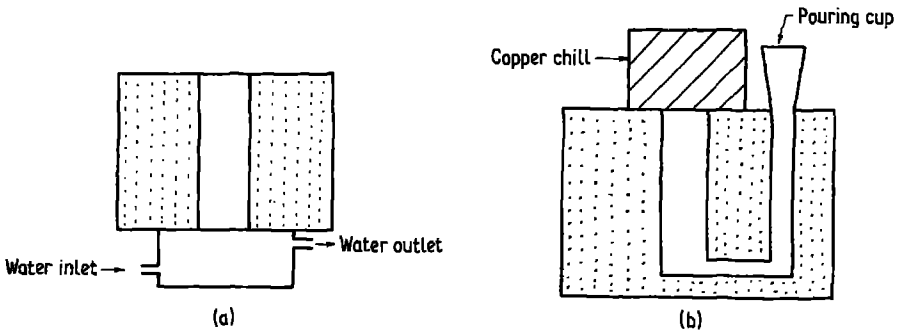

Figure 1 Sand moulds with different chilling arrangements: (a) water-cooled copper chill at the bottom, top-poured; (b) heavy copper chill at the top, bottom-poured.

turntable of a centrifugal casting machine. Details of the casting procedure are given elsewhere [8].

2. Moulds used to obtain a uniform distribution of mica particles:

(i) A cast iron plate mould with a 12.50 mm × 125 mm × 150 mm cavity and 25 mm wall thickness.

(ii) A steel mould as shown in Fig. 2a with a water-cooled copper chill at the bottom also (Fig. 2b).

(iii) A cast iron plate mould with 55 mm × 160 mm × 250 mm cavity and 35 mm wall thickness (pouring temperature 660° C).

Castings obtained after solidifying the composite melts in the above moulds were sectioned, machined and photographed to determine the distribution of mica particles in the metal–matrix composities thus produced.

3. Results and discussion

It was generally observed that mica-dispersed aluminium alloys solidified in permanent moulds showed segregation of most of the mica particles towards the upper portion of the casting. Such segregation is indicated by the macrophotograph of the longitudinal section of a 50 mm diameter permanent-mould cast aluminium alloy–mica particle composite (Fig. 3). This figure indicates that the central bottom portion of the casting is free from mica particles right up to the shrinkage cavity, and thereafter the height of the particle-free zone decreases as one moves towards the periphery of the casting. The segregation (as shown in the later portion of the paper) results from the flotation of mica particles in liquid aluminium alloy. The observed rate of flotation of mica particles is much higher than that calculated using Stokes's law. This deviation might be resulting from partial wetting of these particles by the liquid alloy. Mica is only partially wetted by the liquid aluminium alloys, which results in poor bonding between the particle and the matrix as reflected in poor strength as well as peeling off of mica particles during metallographic polishing (Fig. 4). It was found that the tensile strength of the matrix alloy was reduced by about 50% as a result of the addition of 2.2 wt % mica. This drastic lowering of strength is due to poor bonding between the particle and the matrix resulting in void formation at the particle–matrix interface (Fig. 5), under tensile loading of the composite.

Experiments were conducted under different heat flow configurations in order to determine the tendency of mica to segregate in the cast structure.

In the first experiment, mica-dispersed alloy melt was poured into a sand mould having a water-cooled copper chill at the bottom. Under this arrangement heat dissipation during solidification occurs in a direction opposite to the buoyancy force on mica. A longitudinal section of this casting (Fig. 6) reveals that all the particles have floated to the top portion.

In the second experiment, the composite melt was poured through the bottom of a sand mould having a heavy copper chill at the top. In this case the direction of maximum heat dissipation coincides with that of buoyancy forces, i.e. the solidifying front moves downward while the particles float upward. A macrophotograph of this casting (Fig. 7) also shows mica segregation near the top. It should be noted here that the castings shown in Figs 6 and 7 with mica segregation near the top can find applications where only one surface is subjected to tribological conditions.

Finally, the composite melt was poured into a steel mould, water-cooled from the sides. In this case maximum heat extraction occurs radially, i.e. perpendicular to the direction of mica flotation. A macro-photograph

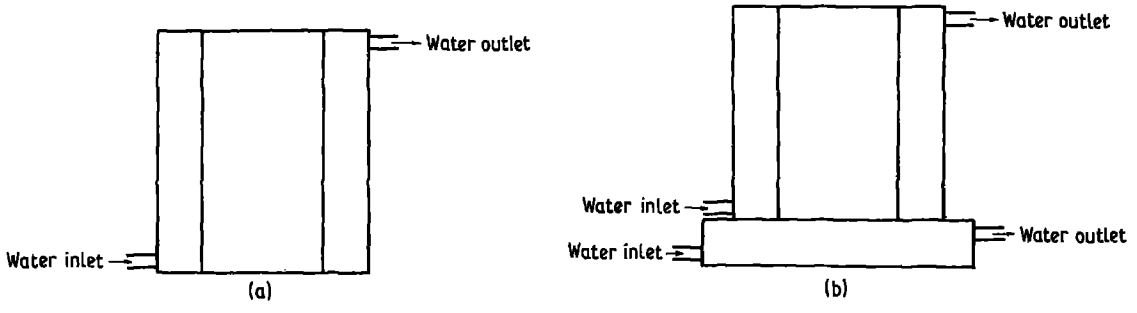

Figure 2 Steel moulds (80 mm internal diameter) with different chilling arrangements: (a) water-cooled from the sides, (b) water-cooled from sides as well as from the bottom.

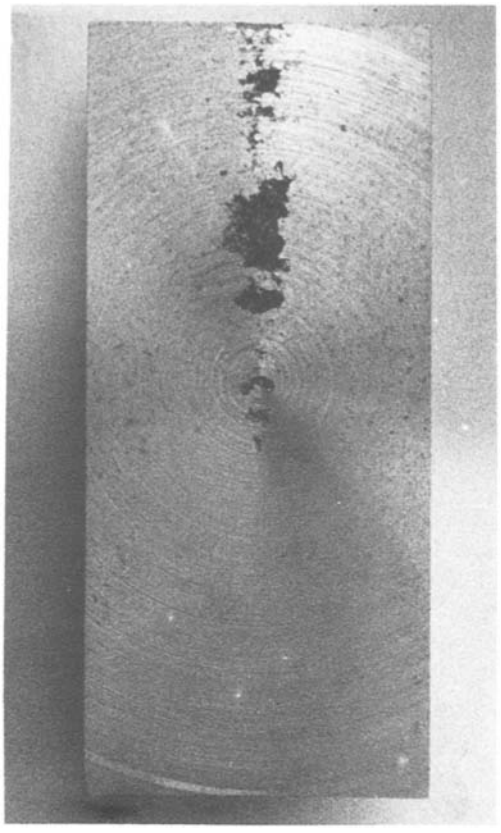

Figure 3 Macrophotograph of the longitudinal section of a 50 mm diameter permanent-mould cast aluminium alloy–mica particle composite (× 0.92).

of this casting (Fig. 8) shows the presence of mica particles up to the bottom along its circumference. However, the central portion of the casting at the bottom is free from mica. The maximum height of the mica-free zone (measured from the bottom of the casting) is found to occur at the centre and decreases progressively as one moves toward the periphery. The central region is the last to solidify and mica gets the maximum time to float up at this location. Calculations of the height of the mica-free zone on the basis of Stokes's law and heat flow considerations show a large discrepancy between actual and theoretical values (see Appendix). Incidentally, it is posible to convert this casting into a plain bearing after machining out the pipe and the central mica-free zone.

Figs 6 to 8 show that mica particles are not pushed

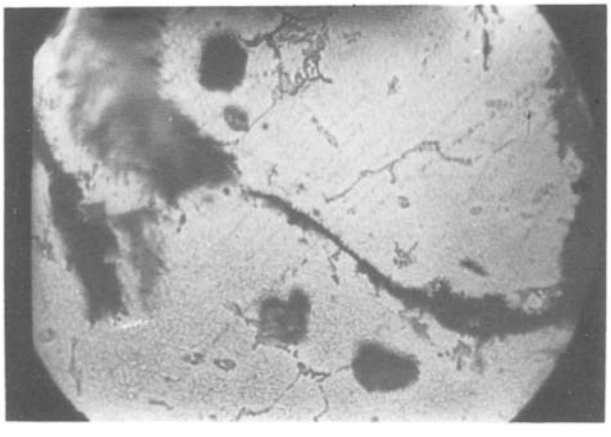

Figure 4 Photomicrograph of aluminium alloy–mica particle composite showing voids due to the peeling off of mica particles (× 210).

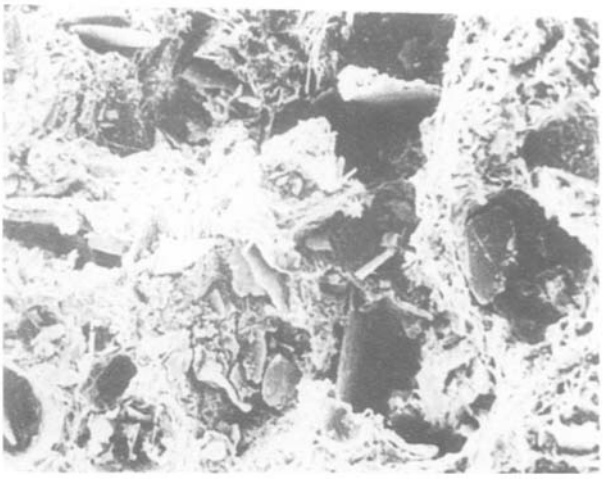

Figure 5 Scanning electron photomicrograph of tensile fractured surface of aluminium alloy–mica particle composite (× 285).

by growing dendrites. Surappa and Rohatgi [10] have proposed a heat diffusivity criteria for the entrapment of particles by a moving solid–liquid front. According to them, in systems in which the factor $(\lambda_P C_P \varrho_P / \lambda_L C_L \varrho_L)^{1/2} > 1$ (P = particle, L = liquid, λ = thermal conductivity, C' = specific heat, ϱ = density), particles are captured by the moving solid–liquid front, whereas for systems in which this factor is less than unity the particles are rejected. For the present aluminium alloy–mica system the heat

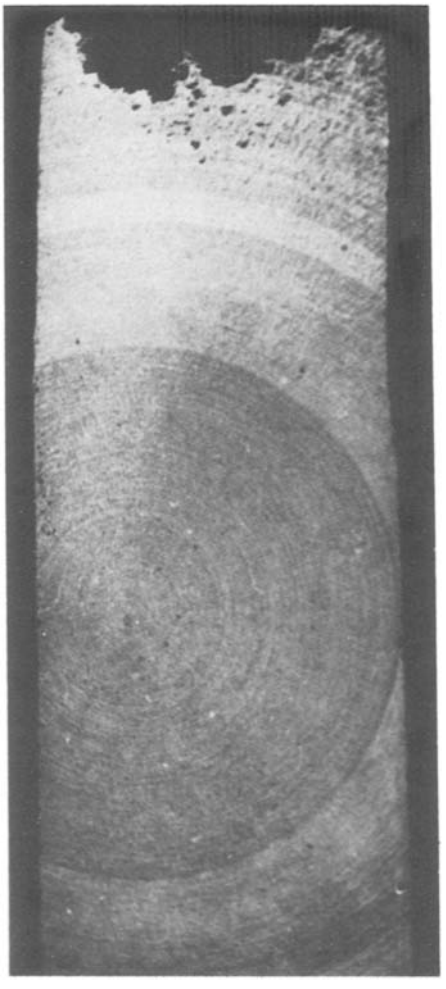

Figure 6 Macrophotograph of longitudinal section of aluminium alloy–mica particle composite casting; poured in sand mould with water-cooled copper chill at the bottom (× 0.85).

Figure 7 Macrophotograph of longitudinal section of aluminium alloy–mica particle composite casting poured in a sand mould with heavy copper chill at the top (× 0.85).

diffusivity criteria shows that mica particles will be rejected by the moving solid–liquid front. However, the heat diffusivity criterion is likely to be valid under conditions where other factors such as body forces do not override the heat flow effects and when the growth rates are very slow [10]. Apparently in the present study several extraneous factors like convection and flocculation seem to be of overriding importance.

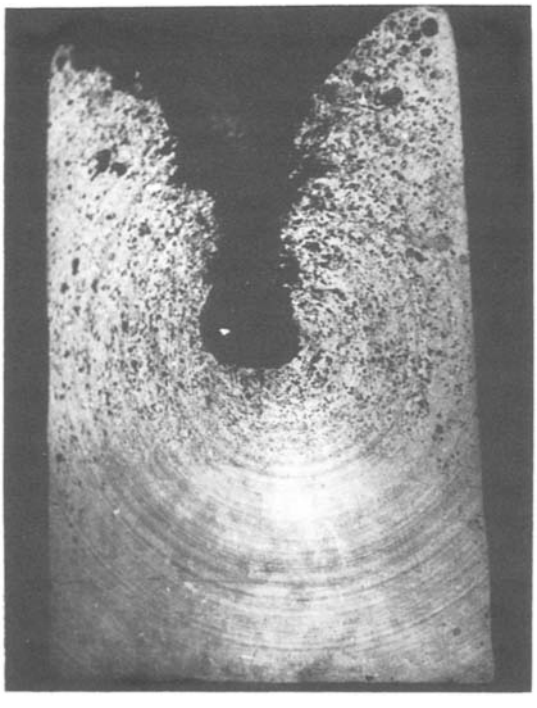

Figure 8 Macrophotograph of longitudinal section of mica-dispersed aluminium alloy solidified in a steel mould water-cooled from the sides (× 0.74).

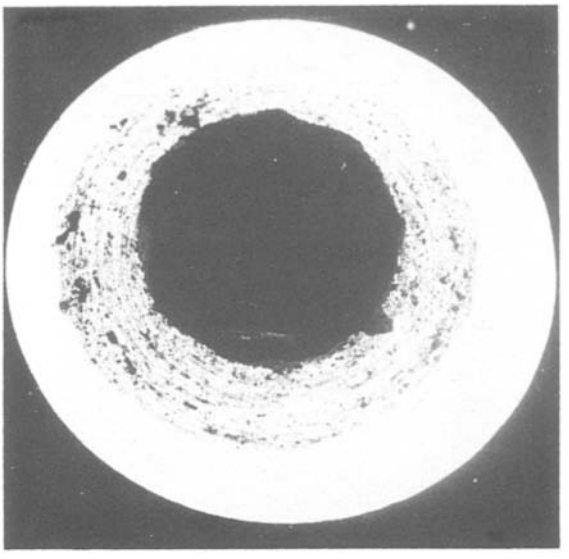

Figure 9 Macrophotograph of radial section of centrifugally cast aluminium alloy–mica particle composite (× 0.75).

Flotation of mica particles under the action of a centrifugal force was also studied. For this purpose the composite melt was cast in a centrifugal casting machine. A macrophotograph of the radial section of the casting (Fig. 9) shows that mica can be moved to surfaces where it is required for tribological applications. The casting in Fig. 9 shows mica segregation toward the inner periphery, which can therefore be suitable for bearing applications. The outer mica-free zone can serve as a good backing material with strength equal to that of the matrix alloy.

4. Methods to obtain a uniform distribution of mica particles

The segregation of mica can be minimized and a fairly uniform distribution obtained by reducing the solidification time of the casting. This can be achieved by

(a) side as well as bottom chilling for large castings;
(b) low pouring temperatures for medium-thickness castings;
(c) making a casting of relatively smaller thickness in general, and
(d) reducing the thickness to be solidified by using cores in cylindrical castings.

A macrophotograph of longitudinal section of aluminium alloy–mica particle composite solidified in an 80 mm diameter steel mould is shown in Fig. 10. This mould was water-cooled from the side as well as the bottom. The figure shows substantial improvement in the distribution of mica particles. Mica particles are seen throughout the section nearly up to the bottom of the casting, which would otherwise have been particle-free right up to the shrinkage cavity.

The casting shown in Fig. 11 was poured at 660° C in a cast iron mould having a 55 mm × 160 mm × 250 mm diameter cavity and 35 mm wall thickness. The homogenous distribution of mica obtained here may be due to reduced solidification time and increased

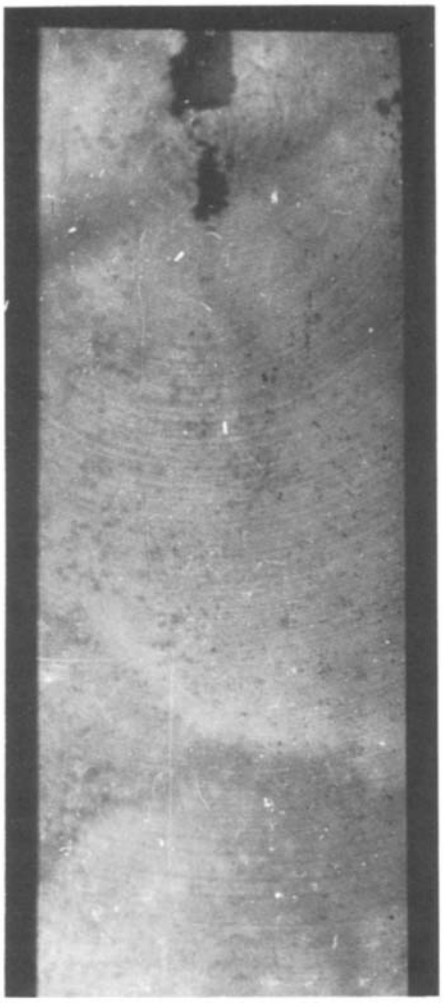

Figure 10 Macrophotograph of longitudinal section of aluminium alloy–mica particle composite solidified in steel mould water-cooled from sides as well as from the bottom (×0.55) (pouring temperature 700° C).

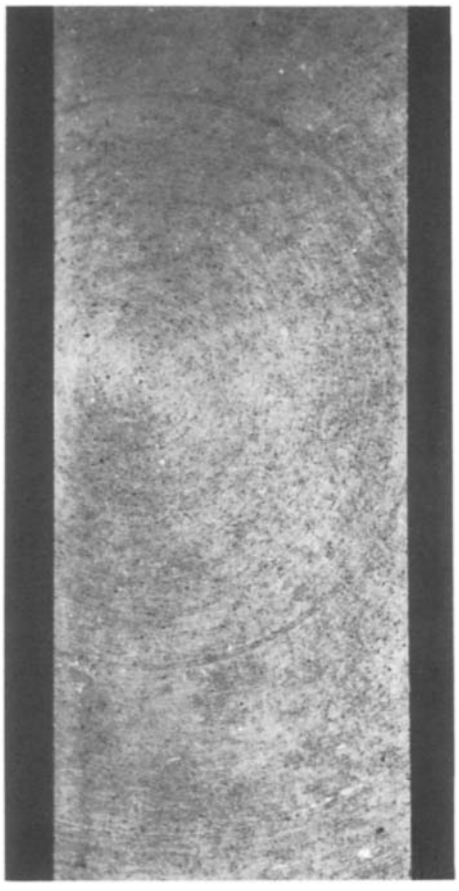

Figure 11 Macrophotograph of a vertical section of aluminium alloy–mica particle composite solidified in (55 mm × 160 mm × 250 mm) plate mould (×0.82) (pouring temperature 660° C).

viscosity of the melt because of the low pouring temperature.

Fig. 12 shows how a reduction in casting thickness can contribute toward homogeneity of the dispersed mica. The casting was obtained in a cast iron mould having 25 mm wall thickness. The melt was poured at 700° C and the freezing time was about 9 sec. The use of a central core can also reduce the solidification time and effect better distribution of particulate matter. Figs 13a and b show longitudinal and transverse sections of a bearing of aluminium–mica composites produced in this manner. For this purpose a central steel core 25 mm in diameter and coated with a clay and graphite mixture was used in a permanent mould (25 mm wall thickness and 50 mm internal diameter). The non-uniform distribution of mica particle obtained in the similar casting produced without using a core may be seen in Fig. 3.

5. Conclusions

1. Castings of aluminium alloy–mica composites show segregation of mica toward the top due to its flotation. The experimental height of the mica-free zone is significantly different from the theoretical value computed on the basis of Stokes's law and freezing-time calculations.

3. A uniform distribution of mica particles can be obtained in castings of smaller section. Thicker castings, however, invariably require chilling and/or low pouring temperatures in order to minimize segregation.

Appendix: Computation of the height of the mica-free zone in an 80 mm diameter casting (steel mould, water-cooled from sides)

It is necessary to calculate the solidification time of the casting and the rate of flotation of mica particles in liquid aluminium alloy to determine the height of the mica-free zone.

An approximate solution for the solid–liquid interface velocity in a water-cooled cylindrical mould has been proposed by Santos and Garcia [11]. The radius–time relationship has the form

$$t = \left[2 - \left(\frac{r_t}{r_0}\right)^2\right]\left[\frac{(r_0^2 - r_t^2)^2\, C_S \varrho_S}{16 r_0^2 \cdot \lambda_S \phi^2} + \frac{\varrho_S (H + C_L \Delta T)(r_0^2 - r_t^2)}{2 h r_0 (T_m - T_0)}\right] \quad \text{(A1)}$$

where

$$\pi^{1/2} \phi \exp(\phi)^2 \operatorname{erf} \phi = \frac{C_S (T_m - T_0)}{(H + C_L \Delta T)} \quad \text{(A2)}$$

where r_t = radius of the liquid region at time t; $2r_0$ = internal diameter of the mould = 8 cm; h = heat transfer coefficient for mould–metal interface = 0.04 cal cm^{-2} (° C)$^{-1}$ = 0.17 J cm^{-2} K^{-1} sec^{-1}; H = latent heat of solidification = 0.945 × 92.4 +

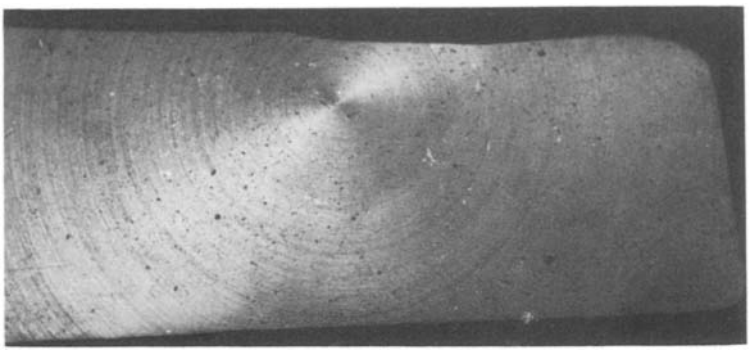

Figure 12 Macrophotograph of longitudinal section of 12.5 mm thick plate of aluminium alloy–mica particle composite (× 0.65).

$0.40 \times 43 + 0.015 \times 46.5 = 88.6\,\text{cal gm}^{-1}$ (92.4, 43 and 46.5 cal gm^{-1} are the heats of fusion of aluminium, copper and magnesium respectively); $\varrho_S = 2.77\,\text{cm}^{-3}$ (S = solid); $C_S = 0.24\,\text{cal g}^{-1}(^\circ\text{C})^{-1} = 1.00\,\text{J g}^{-1}\text{K}^{-1}$; $\lambda_S = 0.37\,\text{cal cm}^{-1}(^\circ\text{C})^{-1}\text{sec}^{-1} = 1.55\,\text{J cm}^{-1}\text{K}^{-1}\,\text{sec}^{-1}$. Equation A2 was solved graphically to determine ϕ; here $\phi = 0.645$.

Using these data in Equation A1, the radius–time relationship can be given as

$$t = \left[2 - \left(\frac{r_t}{4}\right)^2\right][0.0169(16 - r_t^2)^2 + 1.906(16 - r_t^2)] \quad \text{(A3)}$$

The total solidification time from the above equation for an 80 mm diameter casting will be 70 sec.

The rate of flotation of mica particles can be determined by Stokes's equation, according to which their terminal velocity (u) is given as

$$u = \frac{2}{9}\frac{\Delta\varrho g r^2}{\eta} \quad \text{(A4)}$$

where $\Delta\varrho$ = density difference between the liquid and the particle = 2.77 − 2.70 = 0.07 g cm^{-3} and η = viscosity of the liquid alloy = 0.045 poise = 4.5 mPa sec.

Equation A4, which is valid for spherical particles, has to be modified for mica discs which move slower than a sphere of equivalent radius. It has been reported [12] that the ratio of the radii of plates and spheres moving with the same velocity in a liquid will be 2.16, 3.05 and 3.75 for plates of thickness-to-diameter ratio of 1/10, 1/20 and 1/30, respectively.

The surface area of the mica particles was experimentally found to be 2325 $\text{cm}^2\,\text{g}^{-1}$. For diameter of mica disc = 40 μm, equating the experimental value of the surface area to the theoretical value the thickness t was found to be 3.7 μm. Therefore the radius of a sphere moving with the same velocity as a 20 μm radius plate will be 20/2.16 μm.

Finally, substituting these values in Equation A4, the free flotation velocity of mica particles in liquid Al–4% Cu–1% Mg alloy was calculated to be $2.914 \times 10^{-3}\,\text{mm sec}^{-1}$.

The times of solidifications of varying thicknesses of casting were calculated using Equation A3, and the heights of mica-free zones were calculated using these times and the flotation velocity ($2.914 \times 10^{-3}\,\text{mm sec}^{-1}$). These heights of mica-free zones have been plotted at a magnification of ten in Fig. 14, which represents the calculated profile of a mica-free zone. The actual (experimental) profile of the mica-free zone from Fig. 7 has also been plotted in Fig. 14. This figure indicates that although the actual profile of the mica-free zone has the same form as the calculated one, there exists a large discrepancy between the magnitudes of the corresponding heights. For instance, the computed height of the mica-free zone at the centre of the casting in Fig. 13 is $70 \times 0.2914 \times 10^{-3} = 0.0204$ cm, while the measured value is about 3.8 cm.

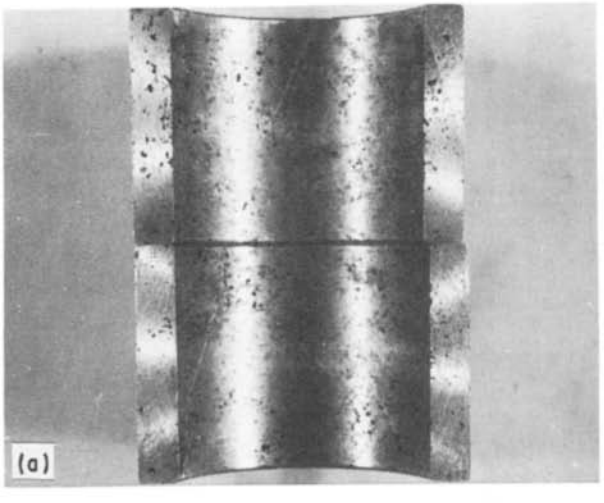

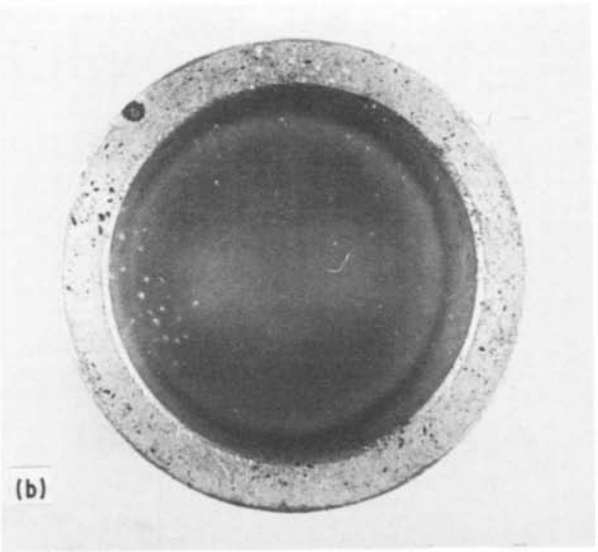

Figure 13 Macrophotograph of (a) longitudinal (× 1.0) and (b) transverse (× 1.45) section of bearing made of aluminium alloy–mica particle composite solidified in a permanent mould with a central steel core.

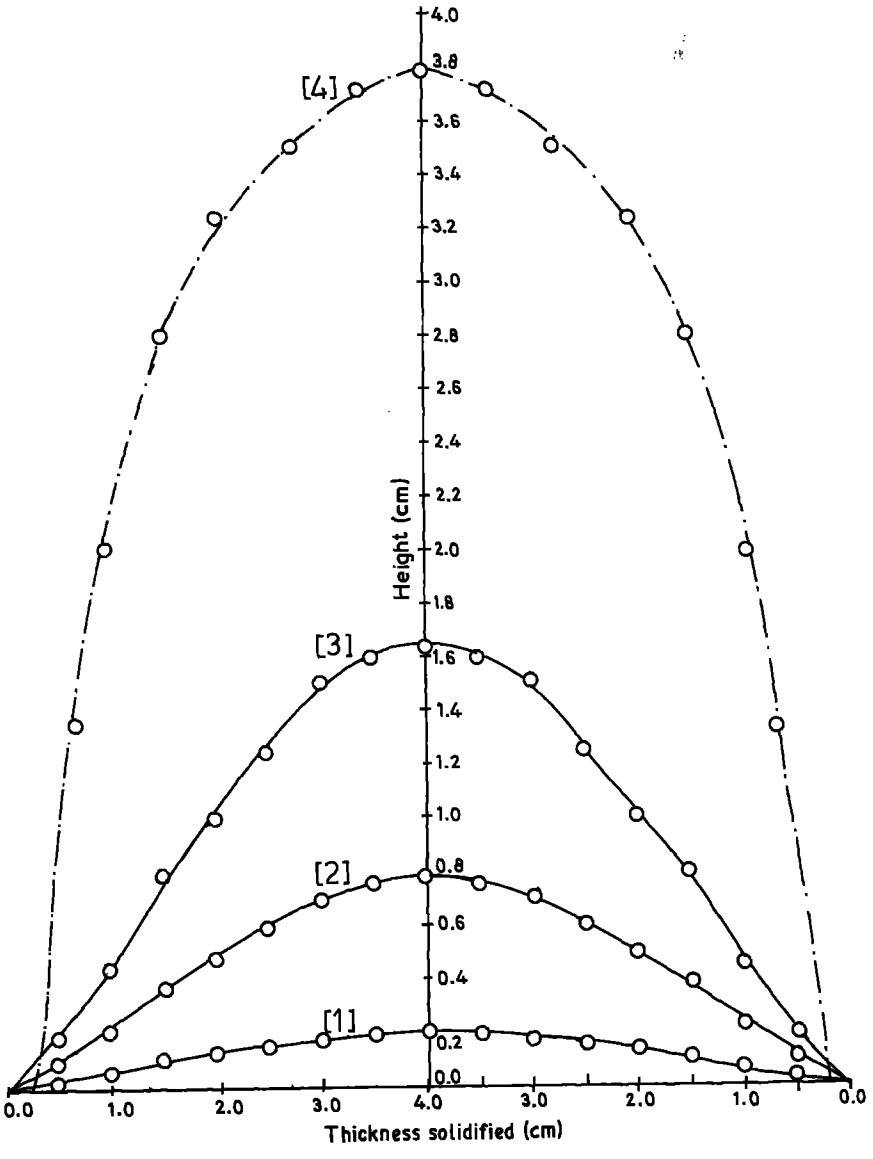

Figure 14 Calculated and actual (experimental) mica-free zone profiles. Theoretical profiles (× 10) for mica particle diameters [1] 40 μm, [2] 80 μm and [3] 120 μm; aspect ratio 1/15; u_t along long axis of particle. [4] Actual profile: water-cooled steel mould; cast LM11–mica (2.0 wt %) composite; mould internal diameter 8.0 μm, length 14.0 cm; pouring temperature 700° C.

References

1. V. F. AFANAS'EV *et al., Fiz. Khim. Mekhan. Mat.* **5** (1969) 680 (Metal Abstracts 7006-620089).
2. V. B. VISHNEVSKII and V. F. AFANAS'EV IZOBERT, *Prom. Obvaztsy, Tovaruye znaski* **45** (1968) 107.
3. M. E. BELITSKII, *Sov. Powd. Metall. Ceram.* **6** (1969) 472.
4. V. N. PAVLIKOV, A. V. TKACHENKIK, A. D. KONDRATENKO and S. C. TRESVYATSKII, *ibid.* **13** (10) (1974) 806.
5. M. E. BELITSKII, *Fiz. Khim. Mekhan. Mat.* **2** (6) (1966) 702.
6. J. ROLLET, Patent Fr 2031 657 (1970).
7. DEO NATH, S. K. BISWAS and P. K. ROHATGI, *Wear* **60** (1980) 61.
8. DEO NATH and P. K. ROHATGI, *Composites* (April 1981) 124.
9. DEO NATH, R. T. BHAT and P. K. ROHATGI, *J. Mater. Sci.* **15** (1980) 1241.
10. M. K. SURAPPA and P. K. ROHATGI, *ibid.* **16** (1981) 562.
11. R. G. SANTOS and A. GARCIA, *ibid.* **18** (1983) 3578.
12. A. M. GAUDIN, "Principles of Mineral Dressing" (Tata–McGraw-Hill, New Delhi, 1977) p. 176.

Received 19 February
and accepted 28 April 1986